Martins, V. S., Kaleita, A. L., & Gelder, B. K. (2021). Digital mapping of structural conservation practices in the Midwest US croplands: Implementation and preliminary analysis. *Science of The Total Environment*, 145191.

Digital mapping of structural conservation practices in the Midwest U.S. croplands: Implementation and preliminary analysis

Vitor S. Martins [a, b*], Amy L. Kaleita [a], Brian K. Gelder [a]

[a] Agricultural and Biosystems Engineering, Iowa State University, Ames, IA, United States.
[b] Center for Global Change and Earth Observations, Michigan State University, East Lansing, MI, United States.

* Corresponding author. E-mails: vitorsm@msu.edu (Vitor S. Martins); kaleita@iastate.edu (Amy L. Kaleita); bkgelder@iastate.edu (Brian K. Gelder)

Abstract

The application of best management practices is a long-term conservation effort in Midwest U.S. croplands, and many farmers have adopted structural conservation practices (SCPs) to reduce soil erosion and surface water runoff, such as terraces and grassed waterways. Despite that, the geographic distribution of these practices is barely known in the region, and mapping initiatives are required to develop timely and spatially explicit inventories of SCP areas. This study presents the first mapping of SCPs in the agricultural areas over 12 Midwest U.S. states. Semantic segmentation model (adapted U-Net) and National Agriculture Imagery Program 2018-2019 data were used to map the SCP areas at 2-m spatial resolution (490.2 billion pixels). In general, mapping results achieved 78.2% overall accuracy across 20 counties. Our results indicate that 52% of SCP areas are distributed over Iowa (26%), Illinois (15%) and Nebraska (11%). In contrast, the states with lowest SCP areas are Michigan and North Dakota, with less than 4% of SCP areas. Since the SCP extent is also dependent on the number of cropland areas per state, the percentage of SCP per cropland area was calculated. Specifically, the average percentage of SCP area per cropland is ~1.19%, ranging from 0.8 (e.g., North Dakota and south Minnesota) to 5.5% (e.g., northeast Kansas and southwest Iowa). Interestingly, results also illustrate that regions with high soil erosion rates present the largest percentage of SCP areas in croplands as well, indicating conservation efforts by farmers. While this preliminary analysis shows some limitations in the mapping quality (mislabel, non-accurate location or discontinuity of SCP areas), the framework has a potential for operational conservation monitoring. The development of such mapping has positive

implications for conservation programs, and this geospatial inventory is an easily accessible information for large-area evaluation of conservation practices across Midwest U.S. croplands.

Keywords: Conservation, terraces, grassed waterways, semantic segmentation, U-net model.

1. Introduction

Agricultural conservation practices are widely recognized across the world (Friedrich et al., 2012; Jat et al., 2013; Kassam et al., 2009; 2019), and the adoption of alternative production methods in farm practices and land management (e.g., no-tillage farming, extensive crop rotations, and biomass mulch soil cover) becomes relevant to maintain soil structure and crop productivity (Triplett et al., 2008; Tscharntke et al., 2012). In the United States, farmers in the Midwest region have implemented conservation practices that benefit both agricultural production and environmental protection (Hobbs et al., 2007; Knowler and Bradshaw, 2007; Kassam et al., 2009; Floress et al., 2018). Despite the efforts to minimize nutrient loss and soil erosion (Carpenter et al., 1998; Schoumans et al., 2014), agricultural non-point source pollution remains a major concern for water quality in the United States (Stoddard et al., 2016). Sediment transport and nutrient export from crop fields lead to degradation of water quality in freshwater systems by increasing algal growth and turbidity levels (Kröger et al., 2013). The Gulf of Mexico “Dead Zone” is one example of the ecological impact caused by nutrient-laden water from the Mississippi River reaching the coastal waters (Rabalais et al., 2002; Diaz and Rosenberg, 2008; Dale et al., 2010). As a result, the U.S. Environmental Protection Agency established a goal of 45% reduction of nutrient loads (nitrogen and phosphorus) to surface waters along the Mississippi basin (Dale et al., 2010). In these efforts, USDA Natural Resources Conservation Service has provided financial and technical assistance for adopting best management practices (BMPs) at farm-level.

Agricultural BMPs are a set of guidelines, practices, and structural controls designed to preserve soil and water resources in agricultural fields. Some examples of structural conservation practices (SCPs) are i) grassed waterways, ii) contour buffer strips, iii) terraces, iv) filter strips, v) riparian buffers, and others. These practices are typically implemented in the most sensitive areas (e.g., highly erodible lands), and each of them has a specific role in the agricultural landscape. For instance, terraces are earthen ridges around a hillside that prevent soil erosion on steep slopes (Tarolli et al., 2014), while grassed waterways are natural or constructed vegetated channels that control surface runoff, erosion, and nutrient loss in the drainage pathways (Fiener and Auerswald, 2003). Recent studies have quantified the benefits of these BMPs in cropland areas (Zhang and Zhang, 2011; Reimer et al., 2012; Liu et al., 2013; Liu et al., 2017). Kröger et al. (2012) reviewed BMP effectiveness in row-crop agriculture over the Lower Mississippi Alluvial Valley and they demonstrated that nine BMPs provide a significant reduction of nutrient loss (range: 15 - 100%), such as total nitrogen and phosphorus. Similarly, Panagopoulos et al. (2011) showed that filter strips reduce the delivery of total phosphorus (up to 50%) in the surface water of a Western Greece catchment. In a modeling approach, Haas et al. (2017) showed that buffer strips reduce nitrate loads reduction (up to 10%) in the catchment of the river Treene, Given the relevance of conservation techniques (Liu et al., 2017; Xiong et al., 2018), conservation agencies and research organizations are promoting local networks and access to information to increase the engagement of farmers towards sustainable practices (Baumgart-Getz et al., 2012), such as North Central Region Water Network (https://northcentralwater.org/) and Iowa Learning Farms (https://www.iowalearningfarms.org/).

In this perspective, the accurate mapping of structural conservation practices becomes crucial for the spatial overview of current practices and its function in the agricultural landscape. Recently, the Agricultural Conservation Planning Framework (ACPF) was implemented to provide meaningful conservation plans at the watershed level (Tomer et al., 2015; Lewandowski et al., 2020). The framework incorporates geospatial data to identify vulnerable areas and recommend conservation options. However, existing practices are not considered in this framework, and the watershed plan often targets areas with already implemented BMPs. Rundhaug et al. (2018) compared the existing and potential ACPF practices in three Iowa watersheds, and they emphasized the importance of BMP mapping as support in the development of conservation scenarios. Regarding the soil erosion modeling, Panagos et al. (2015) highlighted that conservation practices are typically neglected in the soil erosion risk modeling because they are difficult to assess and quantify for large areas. Conceptually, assuming no conservation or constant values, significant uncertainties may be introduced in the erosion estimates, especially in agricultural areas. These examples show the benefits of geospatial information of conservation practices for environmental analysis, but mapping initiatives are barely presented in the literature. In this context, Iowa BMP Mapping Project (IBMP) is a unique initiative that offers a detailed spatial database about vegetative/structural practices across Iowa watersheds (ISU, 2016). The mapping framework includes the visual interpretation of National Agriculture Imagery Program (NAIP) aerial imagery (2007-2010) and LiDAR-derived products. While a comprehensive inventory is a valuable data resource (Lam et al., 2011; Rundhaug et al., 2018), the product generation is dependent on manual classification performed by multiple GIS specialists/interns and takes multiple years for completion. This limitation reinforces the demand for a timely and reliable framework for SCP mapping which will support the evaluation of other U.S. states.

This study evaluates the preliminary results of structural conservation practices (SCP) mapping across Midwest U.S. croplands. The framework includes the classification of SCP areas using high-resolution NAIP aerial imagery (2018 – 2019 and semantic segmentation U-Net algorithm). The classification was performed over ~490.2 billion pixels at 2-m resolution, and the computational strategies for efficient implementation were detailed in this study. The results of SCP areas were reported by state, and then, normalized by cropland area for further evaluation of its spatial distribution. In addition, we investigated the relationship of high\low occurrence of SCPs with landscape characteristics, such as soil properties and topographic-related variables. Note that agricultural BMPs represent a variety of conservation practices (cover crops, nutrient management, crop rotations and tillage practices), and this study is only focused on structural practices, such as terraces and grassed waterways. These preliminary results are promising, and the potential implications and challenges were discussed in the Section 4.

2. Material and methods

The proposed framework applies publicly available imagery (NAIP) and semantic segmentation U-Net method to generate a SCP/non-SCP mask in agricultural areas. The U-Net is a deep learning model that explores spatial-spectral features for image classification and further details are presented in the section 2.3.1. The procedures are shown in Fig. 1 and broadly described as: 1) NAIP pre-processing; 2) model training; 3) SCP classification and 4) validation and spatial analysis. These steps are detailed in the following sub-sections.

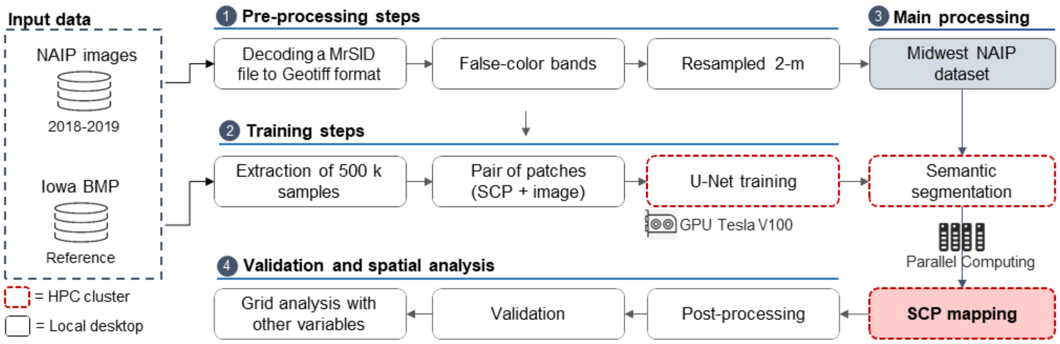

Fig. 1. Framework for structural conservation practices (SCP) mapping using deep learning model.

2.1. Study area

The study area includes one of the major cropland areas in the world: Midwest United States. A total of 12 states were selected for this analysis, and they represent the most grain productive region of the United States (Table S1). For example, Iowa is a leader of U.S. corn production (68.5 million tons of corn) with approximately 87,500 farms (Iowa Corn, 2019). The region presents mostly a hot-summer humid climate and cold winters, and commercially and environmentally relevant U.S. rivers are crossing the region such as Mississippi and Missouri rivers. While cropland areas are the most predominant land cover, the natural landscape consists of prairie and savanna, forests, and wetland areas. The terrain landscape is typically flat or moderately rolling hills such as in southwest Wisconsin or western Iowa. The frequency of corn/soybean areas illustrates the importance of selected states for national crop production (Fig. 2), and consequently, the conservation efforts are highly expected in this region.

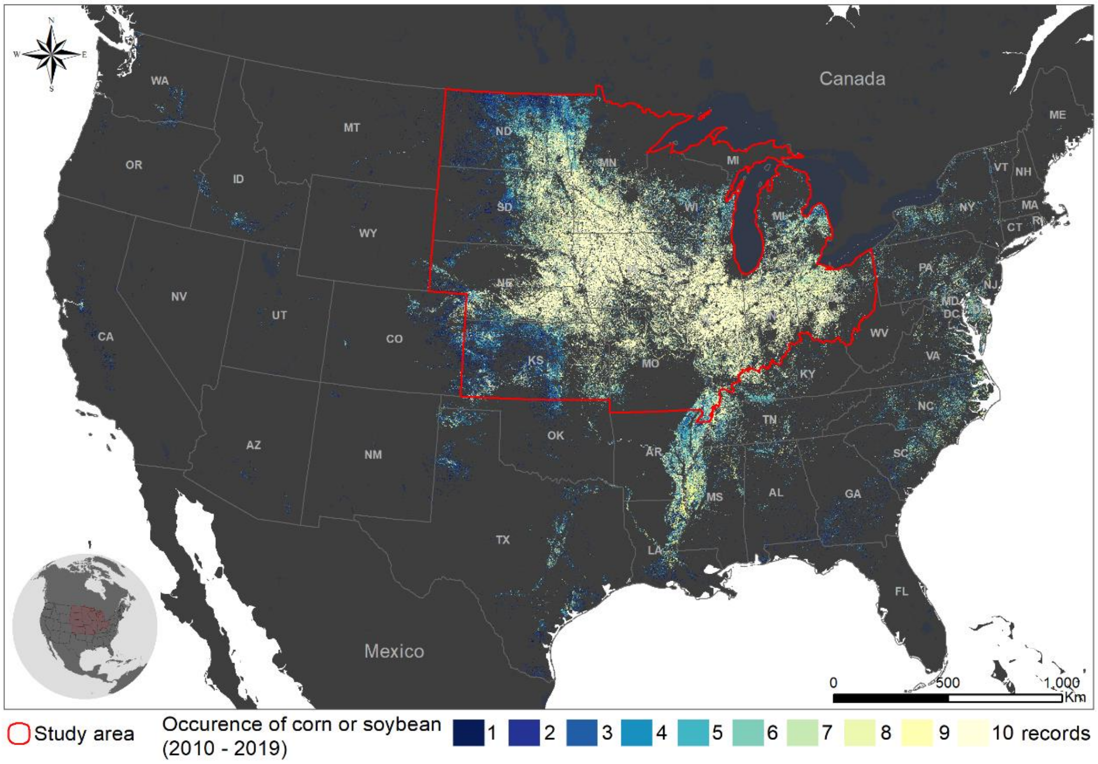

Fig. 2. Location of Midwest U.S. states (study area). The crop frequency of corn\soybean is colored from dark blue (1 year) to light yellow (10 years) in the 2010-2019 period. Source: https://nassgeodata.gmu.edu/CropScape/.

2.2. Data

2.2.1. High-resolution aerial imagery

National Agriculture Imagery Program (NAIP) is a comprehensive program administered by the USDA's Farm Service Agency (FSA) that acquires high-resolution aerial imagery across the United States. The NAIP imagery are mostly collected during the agricultural growing season (leaf-on) and have the appropriate resolution for a variety of land cover and environmental studies (Basu et al., 2015; Peter et al., 2018; Martins et al., 2020). Beginning in 2003, NAIP projects were developed on a 5-year cycle to collect images at natural color (RGB) using film cameras. Recently, NAIP imagery are acquired by digital sensors with four spectral bands (blue, green, red and near-infrared), 8-bit of radiometric resolution and spatial resolution of 1-m. The clear-sky images are collected on different flight dates during late summer and early fall and provided for public as orthorectified imagery for each U.S. county. The dataset is available by USDA Natural Resources Conservation Service at Geospatial Data Gateway (Direct download: https://nrcs.app.box.com/v/naip).

In this study, false-color NAIP imagery were obtained for entire Midwest U.S in 2018 and 2019. A total of 1,054 county-based image were delivered in MrSID compressed format, resulting in ~1.98 TB of data. For the pre-processing step (Fig. 1), these images were decoded to GeoTiff format and then resampled from full 1-m resolution to 2-m resolution using nearest neighbor method. This resampling reduces the storage needs and keeps sufficient resolution for our analysis. After that, the entire dataset was re-projected to USA Contiguous Albers Conic Equal Area (ESRI:102003). Note that this study does not perform a temporal analysis because older NAIP images present different number of bands and image quality compared to recent data. Also, we did not use the LiDAR-derived product as input variable because they are not available at high spatial resolution (< 2 m) for all states. Moreover, state-based LiDAR products are often distinct in terms of pre-processing steps, vertical error, project's year, spatial extent, and final quality. The uncertainties of different data sources and its coverage restrict the model application for entire Midwest, so then, we decided to only use false-color NAIP images. Additional discussion of current limitations is presented in Section 4.4.

2.2.2. Reference samples for model training

The development of large training datasets is one of the major challenges for deep learning applications. The training of semantic segmentation methods, such as U-Net model (Section 2.3.1), requires fully labeled image patches, and this study exploits the Iowa BMP dataset to generate these training samples (Fig. S1). As described, the Iowa BMP project has been funded by multiple institutions and produced a BMP inventory in geodatabases for the 2007-2010 timeframe. The Iowa-BMP is focused on a baseline of conservation practices, such as terraces, WASCOB, grassed waterways, strip cropping and contour buffer strips. The project developed a protocol for visual interpretation of BMP areas using optical image and LiDAR-derived products, and later, the quality assessment is performed by trained Iowa-DNR staff before data release. Therefore, this dataset is reference source for a variety of environmental assessment, and the complete set of BMPs is available at watershed-level through the project's website (https://www.gis.iastate.edu/gisf/projects/conservation-practices). Further information is also provided in the project handbook (ISU-IBMP, 2017). Among these BMPs, this study investigates two relevant structural conservation practices (SCPs): grassed waterways and terraces. These practices are the most abundant in the Iowa inventory (> 90% of areas in BMP project), and they are typically observed within cropland boundaries. Here, it should be emphasized that these practices are visually identified in the images, but they are difficult to separate using optical data due to similar spectral response and shape in some cases (even by human interpretation). So, binary classification (SCP/non-SCP) is appropriate for this study, and this limitation is further discussed in Section 4.4. For this training dataset, SCP polygons were firstly converted to raster files, creating a binary label (SCP: 1, non-SCP: 0). All these labeled patches are stored with corresponding false-color images from NAIP 2010 data, as used in the Iowa BMP project. The next step was the random selection of 500,000 pair samples (image + label), where 90% of these samples have SCP areas and the other 10% of samples have non-SCP areas, such as grassland, building, road and forest targets. This combination of SCP and non-SCP patches gives a comprehensive dataset (size: 122 GB) for model training, and this dataset is publicly available at https://doi.org/10.5281/zenodo.3762370.

2.3. Methodology

2.3.1. Semantic segmentation with deep learning

Recently, fully convolutional network became a prominent deep learning architecture for semantic segmentation tasks (Long et al., 2015; Ronneberger et al., 2015; Badrinarayanan et al., 2017; Jégou et al., 2017). These architectures are well-established in remote sensing applications and have been used to map land cover (Stoian et al., 2019), forest degradation (Wagner et al., 2020), building (Xu et al., 2017) and roads (Zhang et al., 2017). A detailed review of different studies is described in Ma et al. (2019). In this research, an adapted U-Net network was used to perform a binary segmentation of a vegetative/structural SCP areas. Briefly, U-Net is a deep fully convolutional network that was originally designed for semantic segmentation of biomedical images (Ronneberger et al., 2015). This model presents the advantage of 2D feature extraction to explore spatial-contextual information compared to standard pixel-based methods (e.g., random forest and support vector machine). The U-Net has an encoder-decoder architecture where (i) the encoder part extracts spatial features from the input image and (ii) decoder constructs the segmentation map from the encoded features. By following Wagner et al. (2020), we adapted the U-Net architecture with three-band input image and additional convolutional block to explore deeper features of our large training dataset. Furthermore, we added batch normalization and dropout layers to prevent overfitting in each block. In general, our network contains five blocks with two convolutional (3 x 3) layers followed by ReLU activation function and max pooling (2 x 2) in the encoder part. In the decoder part, a sequence of upsampling and convolutional layers reconstructs the dimension of input patch until the end of network. Finally, the last layer has convolutional layer (1 x 1) with sigmoid activation function and generates the confidence map with the same dimension of input. The SCP label is attributed to pixels with output layer values higher than 0.5.

The adapter U-Net model was trained with 500,000 image patches. The first 90% of the dataset is used for training (450,000 patches), while the last 10% is used for validation (37,500 patches) and testing (12,500 patches). For network training, a custom data generator was designed to feed the model (batch-by-batch) because there is not enough memory to load all the 500,000 samples at the same time. We used the Adam optimizer (learning rate = 0.001) and the binary cross-entropy as loss function, which is most appropriate for this segmentation task. The number of epochs was set as 100 (batch size of 32) since the improvement did not exceed 0.002 of accuracy after 80 epochs. This model was trained in the ISU HPC Pronto cluster with Intel Xeon Silver 4114 CPU @ 2.20GHz, and GPU NVIDIA Tesla v100 32GB. Note that this adapted U-Net architecture has 31,099,429 trainable parameters, and large GPU memory is needed for this application. The total training takes up to 13 days (~10,850 secs per epoch). The training, validation, and testing accuracies were similar (0.983, 0.974, 0.975, respectively), which indicates small or no overfitting during the training. All these experiments are conducted with Python's high-level package Keras (TensorFlow backend) in Python environmental and its open-source libraries, such as GDAL, NumPy, and Scikit-image.

2.3.2. SCP classification and post-processing

This product generation demands computational resources for fast processing of large volume of high-resolution data across the Midwest region; more specifically, this study classified ~490.2 billion pixels. In this research, we performed all the classification process in the High-Performance Computing (HPC) Condo cluster at Iowa State University. There are relevant aspects for the efficient processing of these high-resolution images. The county-based images are large files (range: 300 MB to 17 GB) and imposes a high load on the nodes with intense read/write of files and memory limitations for multi-processing jobs. To solve that, the first step was the subdivision of original image in 18 small parts, and then, perform the parallel processing of these small image files. This step takes advantage of multiple cores in HPC nodes and we run dozens of image parts simultaneously using 15 nodes. Another part of patch-based classification is the sliding window process. One of the main advantages of FCNs is the "dense" prediction where all pixels are labeled in the output patch, and this reduces the redundancy in the classification. However, SCPs are typically long and continuous areas, and some overlap is needed to maintain the spatial-contextual features on the border and between adjacent patches. We adopted stride of 192 pixels between input patches (in other words, overlap area equal to 64 pixels) to balance running time and quality of results. Finally, the entire Midwest U.S. is classified in five days (processing time: ~14 min per 100 km^2 of image), generating 1.39 TB of mapping results. After that, a post-processing step is implemented for the final product, including the filter of non-cropland areas and noise areas. The cropland data layer (CDL) from USDA was used to filter the non-cropland areas. The cropland mask was created with corn or soybean areas occurring at least 5 times between 2010 and 2019 (see areas in Fig. 2 with frequency ≥ 5). Since noise and isolated pixels are likely expected at 2-m classification, and we filtered out small areas (up to 20 pixels). Finally, we aggregated all tiles to produce a binary mask (SCP/non-SCP) per county.

2.4. Accuracy assessment

For classification assessment, we developed a reference dataset using stratified random sampling design (Cochran, 2007). Briefly, a total of 9,270 reference samples were labeled in 20 Midwest counties (Fig. S2). In the first step, 250 blocks of 2 x 2 km dimension were randomly created for each county, and then, we choose 50 blocks with high presence of SCP areas as possible. This block-based stratification allows the consideration of spatial variability of SCP areas compared to simple random sampling, which increases the probability of SCP samples in this reference dataset. In the second step, we created five random points for each block and these samples were labeled as either SCP or non-SCP pixels by visual interpretation of high-resolution imagery from NAIP data and ArcGIS image online service. After this step, additional samples were included to match the number of SCP and non-SCP samples per block. When a particular block does not present any SCP on cropland area, this previous step is skipped, and only randomly selected points were labeled. An example of block-based sampling of

SCP and non-SCP pixels is illustrated in Fig. S2. By using 9,270 reference samples, the confusion matrix was calculated in this per-pixel accuracy assessment, including other metrics such as overall accuracy (OA), producer's accuracy (PA), user's accuracy (UA) and F-1 score (Congalton et al., 1991; Strahler et al., 2006).

$$\text{Accuracy} = \frac{TP + TN}{TP + TN + FP + FN} \tag{1}$$

$$\text{Recall} = \frac{TP}{TP + FN} \tag{2}$$

$$\text{Precision} = \frac{TP}{TP + FP} \tag{3}$$

$$\text{F1-score} = 2 \times \frac{\text{Precision} \times \text{Recall}}{\text{Precision} + \text{Recall}} \tag{4}$$

Where, true positive (TP) and true negative (TN) represent the samples that were correctly classified as SCP and non-SCP, respectively. In turn, the false positive (FP) samples are those pixels mistakenly classified as SCP, while the false negative (FN) samples are those pixels mistakenly classified as non-SCP areas. The F1-score uses a harmonic average of the precision and recall metrics, ranging from 0 to 100. Precision is the proportion of classified samples that in fact belong to this class and it is similar to user's accuracy (1 – commission error). Recall is the proportion of reference samples that were classified as SCP locations and it is similar to producer's accuracy (1 – omission error).

2.5. Spatial analysis and ancillary products

The spatial analysis includes the discussion of SCP distribution, spatial autocorrelation (Global Moran's I test), and Local Indicators of Spatial Association analysis. The SCP areas were calculated per grid with regular size (10 x 10 km), and then, Anselin Local Morans I analysis was performed. Furthermore, the adoption of conservation practices is potentially affected by a variety of factors such as soil and terrain properties (Knowler and Bradshaw, 2007), and the association between SCP and some variables was evaluated in the high and low clusters of SCP extent. The used variables are described as follows:

Topographic-related features: The 30-m elevation product from Shuttle Radar Topography Mission (SRTM) was used to calculate the topographic-related features, such as slope and topographic wetness index (TWI). The index calculation is described by TWI = $\ln(A_s/\tan(\beta))$, where A_s is the upslope contributing area, and β is the local slope (Quinn et al., 1995). The SRTM 30-m images were acquired in the web interface (SRTM Tile Downloader, https://dwtkns.com/srtm30m/) for Global Change Master Directory dataset (https://gcmd.nasa.gov). While 30-m SRTM DEM has inherent uncertainties, the data source is well-established in the literature and was used to derive averaged values of slope and TWI within 10 x 10 km grid.

Soil-related features: Saturated hydraulic conductivity (µm/s), bulk density (g/cm^3), and soil organic matter (kg/m^2) were used in this study. These products were distributed by SoilWeb portal (https://casoilresource.lawr.ucdavis.edu/) from California Soil Resource Lab at UC Davis, and they were derived by aggregating USDA-NCSS soil survey data (SSURGO back-filled with STATSGO where SSURGO is not available) within 800m^2 grid cells.

Soil erosion rate: Global Soil Erosion 2012 (tons/ha/yr) and K-factor maps from Borrelli et al. (2017) were used in this study. This 25 km resolution product is a re-sampled version of the original soil erosion map derived from RUSLE-based Global Soil Erosion Modelling platform. The product is available at European Soil Data Centre (https://esdac.jrc.ec.europa.eu/content/global-soil-erosion) (Panagos et al., 2012), and more details of soil erosion mapping are found in Borrelli et al. (2017).

All these variables were re-projected to Albers Conic Equal Area projection and filtered by cropland mask, and the average values of these variables were calculated for each 10 x 10 km grid.

3. Results

3.1. Classification performance and error sources

This section presents the results of accuracy assessment and examples of SCP mapping using semantic segmentation approach. The confusion matrix is presented in Table 1, and the overall accuracy and F1-score of the SCP mapping are 78.2% and 68.5%, respectively. This validation shows large number of false negatives (1927) and low recall of 53.3% which suggest the underestimation of areas in this mapping with high omission error. In turn, the precision of 95.9% and small false positives samples suggest a low commission error. The visual inspection shows some positive aspects of 2-m product (Fig. 3). In the Figs. 3a and 3b, we observed the successful classification of terraces and grassed waterways in different context. For instance, we observed the performance in both vegetated and fallow areas with correct label (Fig. 3b versus 3e) and even in the transition areas. It is worth emphasizing that urban and forest pixels were filtered out by cropland mask, but we did not observe a systematic error in the raw product, and they are typically classified as non-SCP pixels as expected. Another example of SCP mapping illustrates the performance of our results (Fig. S3). In this example, the terrace locations are consistent with contours in hillshade map, and different shapes and dimension of terraces are well-represented.

Table 1. Confusion matrix of SCP mapping across 20 counties.

All states	Overall accuracy: 78.2 %; F1-score: 68.5%				
	Reference				
Classified	Non-SCP	SCP	Total	Recall (%)	Precision (%)
Non-SCP	5048 (TN)	1927 (FN)	6975	53.3	95.9
SCP	94 (FP)	2201 (TP)	2295		
Total	5142	4128	9270		

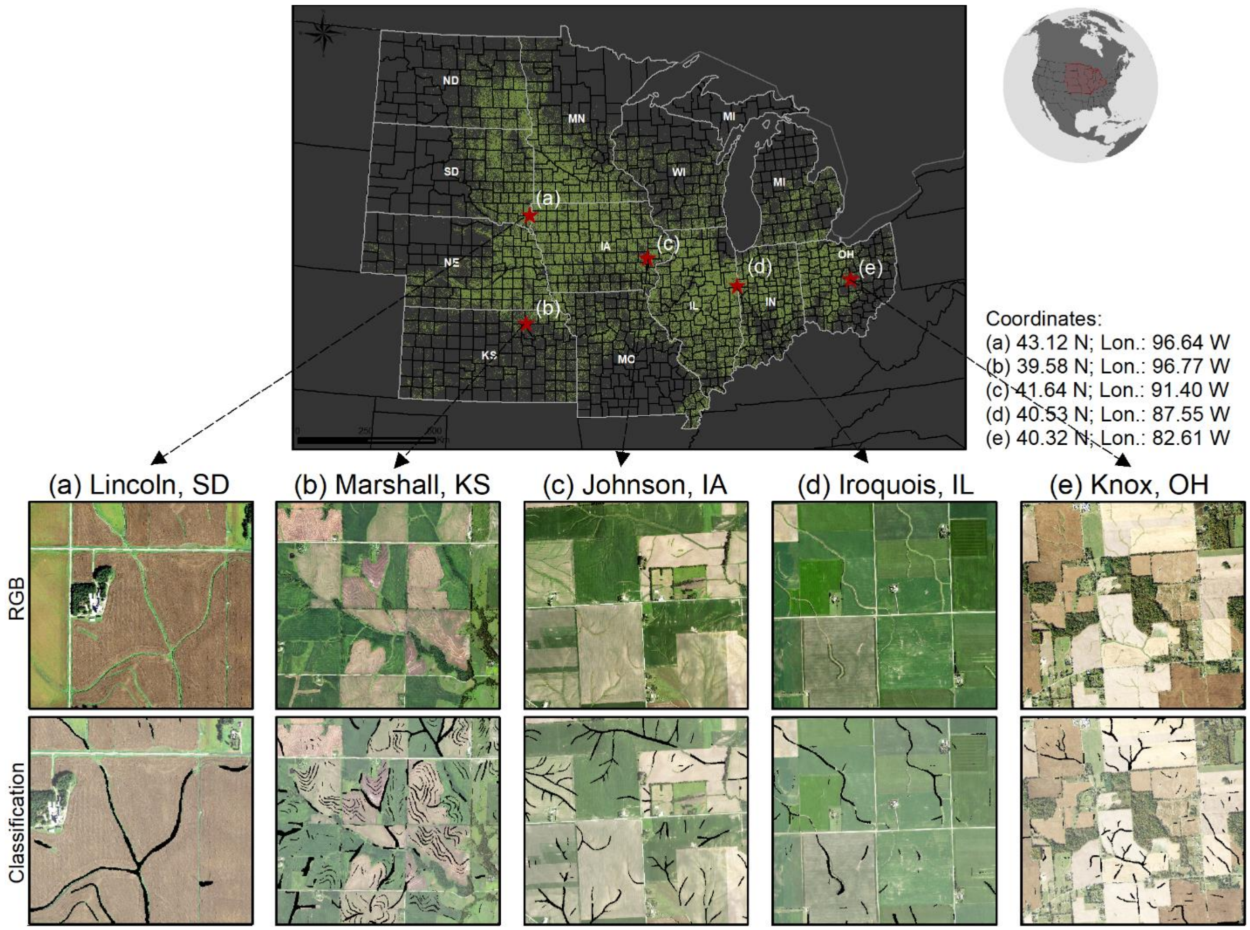

Fig. 3. Classification of structural conservation practices (SCP) in different contexts (a-e). *First row*: NAIP natural color image. *Second row*: SCP mapping (black).

While this overall accuracy can be claimed as satisfactory for this general analysis, the farm-level analysis is potentially affected by omission/commission errors. Fig. S4 shows some limitations of this mapping. For example, the discontinuity of SCP area is one of the most common omission errors, where the grassed waterway is partially mapped, or terraces are missed (Fig S4a). In fact, as suggested in the confusion matrix, the omission of SCP area is the main error source in this mapping and can lead to certain underestimation of SCP areas. In another way, the commission error is also observed in the regions where the crop surfaces are visually complex and quite heterogeneous. We observed that wetter areas present erroneous mislabels of SCPs in the crop field. Such errors are expected as the model performance is dependent on clear distinction of spatial pattern between SCP and non-SCP targets. In the same context, it should be emphasized that irrigated areas are not common practices across Iowa, which makes it poorly represented in the training samples. As consequence, we found a critical confusion of SCP areas in the central pivot irrigation areas where the pivot wheel path or edges of irrigated areas are confused as conservation practice (Fig. S4b). Lastly, the flooding farmlands present complex water paths, and some errors were observed in North Dakota and Wisconsin. Despite these aspects, this preliminary analysis shows sufficient quality for overview analysis of SCP distribution across the U.S. Midwest.

3.2. SCP distribution in the Midwest U.S.

Fig. 4 shows the absolute SCP areas per state and the number of funded terraces and grassed waterways by NRCS conservation programs between 2005 and 2019. In general, a total of 6,642 km^2 was classified as SCP areas in the cropland across the entire region. We observed that 52% of SCP areas are distributed over Iowa (26%), Illinois (15%) and Nebraska (11%). The states with lowest SCP areas are the North Dakota and Michigan, with 4% of total. The largest SCP areas and practice counts are both observed in Iowa, which might indicate the importance of these programs towards achieving conservation goals. Interestingly, we observed several terraces across Kansas but there are no records of NRCS funding for this practice during 2015-2019 period. The small SCP areas in North Dakota and Michigan also agrees with low number of NRCS records for terrace/grassed waterways projects. This overview of classified SCP and NRCS records is relevant to discuss the effectiveness of cost-share programs.

Regarding the spatial distribution, the evaluation of SCPs requires the normalization by cropland areas. For this reason, we calculated the percentage of SCPs per cropland area, and spatial distribution of % SCP is shown in Fig. 5a. In addition, Local Moran’s I cluster map and cropland mask are presented in Fig. 5b and Fig. 5c, respectively. The map shows the grids with higher than 10% of cropland within 10 x 10 km. Overall, the values range from 0 to 8% of SCP in croplands and the spatial distribution indicates large variability of % of SCP and different conservation efforts across the states. For example, the largest extent is clearly observed in the western and eastern Iowa, while north central Iowa, also known as Des Moines Lobe due to its post-glacial landscape, has low SCP areas (< 1%). Interestingly, Ohio shows more than 1% in the middle of state, but the rest of state has lower than 0.8% of SCP in croplands.

Southern Minnesota, Michigan and North Dakota represent the areas with lowest % of SCP. In turn, Illinois shows similar distribution of % SCP percentage across state. By visual inspection, we observed that classified SCPs in northeastern Kansas are mainly terraces, which highlights the conservation needs in this region. In addition, the cluster and outlier analysis is also illustrated in the same Fig. 5. The Global Moran's I shows a spatial autocorrelation of % SCP values (clustered, p-value < 0.05) and clustering results demonstrate that high-high clusters occur in large extent over Iowa, Kansas and Nebraska. As a hotspot region, the gridded SCP areas present high similarity with their neighbors, and average SCP percentage of 2.65% (± 0.73) is observed in the high-high cluster. In contrast, North Dakota, Minnesota and Michigan present most areas of low-low clusters, which indicate fewer efforts (or no need) in the SCP implementation.

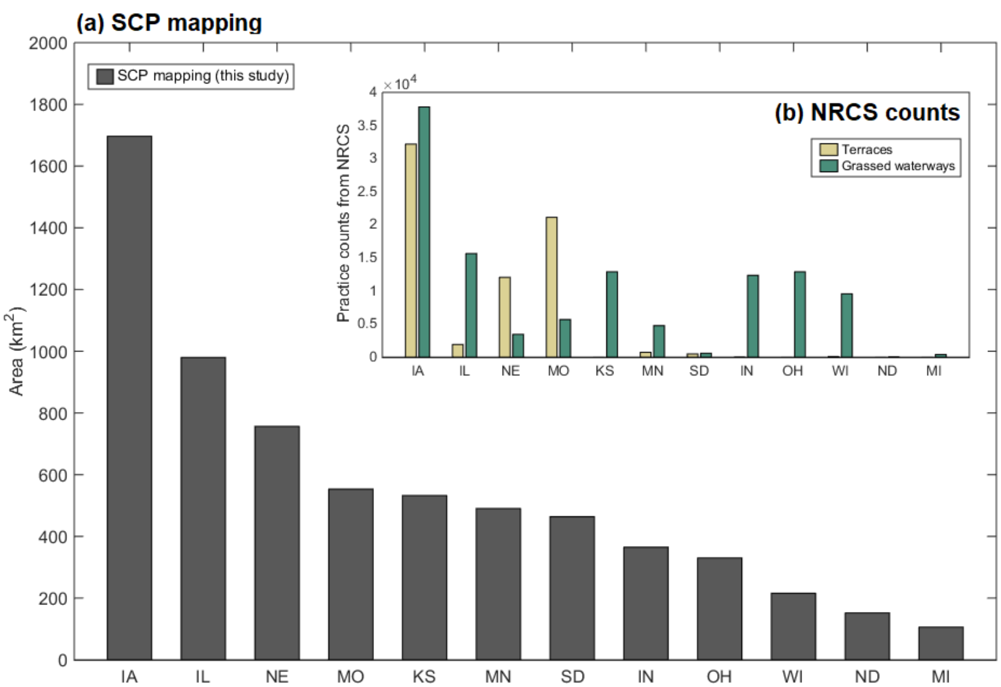

Fig. 4. (a) Comparison of structural conservation practices (SCP) areas among the U.S. states. (b) Numbers of grassed waterway and terrace practices funded by Natural Resources Conservation Service (NRCS) in 2015-2019 period. Source: https://www.nrcs.usda.gov/Internet/NRCS_RCA/reports/, (e.g., "cp_ia.html" for Iowa). U.S. state abbreviations: Illinois (IL), Indiana (IN), Iowa (IA), Kansas (KS), Michigan (MI), Minnesota (MN), Missouri (MO), Nebraska (NE), North Dakota (ND), Ohio (OH), South Dakota (SD), Wisconsin (WI).

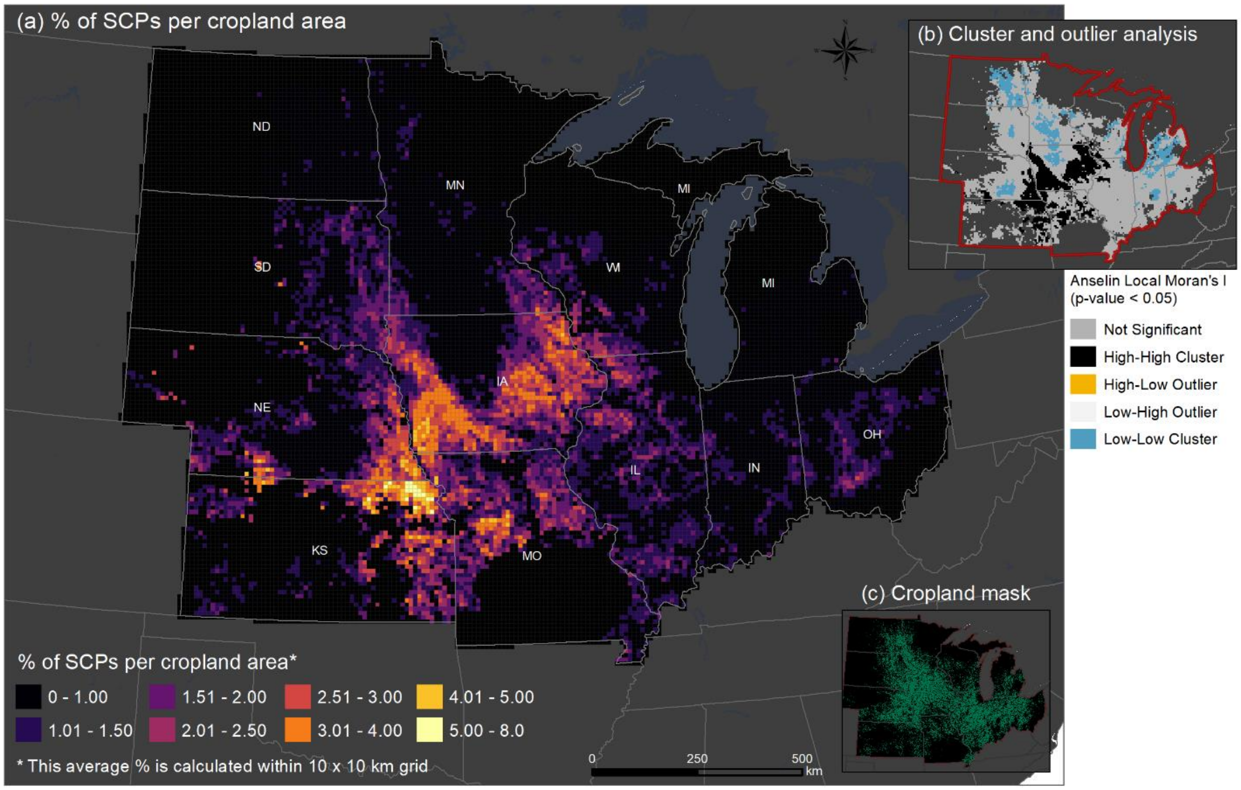

Fig. 5. (a) Spatial distribution of structural conservation practices (SCP) in terms of percentage within agricultural areas across Midwest U.S. region. (b) Results of cluster and outlier analysis (Anselin Local Moran's I) at 5% significance level. (c) Cropland mask. Note that average % of SCPs is calculated within 10 x 10 km grid area, and only grids with more than 10% of cropland mask are used in this map. U.S. state abbreviations: Illinois (IL), Indiana (IN), Iowa (IA), Kansas (KS), Michigan (MI), Minnesota (MN), Missouri (MO), Nebraska (NE), North Dakota (ND), Ohio (OH), South Dakota (SD), Wisconsin (WI).

3.3. Relationship between SCP and other variables

The evaluation of soil and topographic variables in the areas with SCPs supports the understanding of motivations to adopt these practices. Fig. 6 shows the histogram of six soil/topographic variables obtained over high-high and low-low cluster areas of SCPs (%). From Anselin Local Moran's I analysis, high-high clusters represent the grids with high % of SCP where its neighbors also present high values, while low-low clusters are the same idea but low % of SCP values. In general, high-high clusters of % SCP are observed in slope (average = 1.58%), TWI (4.45) and Ksat (6.68 µm/s) compared to low-low clusters with slope of 0.75%, TWI of 5.07 and Ksat of 19.8 µm/s. Also, there are slight differences in the k-factor, bulk density and SOM values between high-high and low-low clusters. While these results suggest some relationship of these soil/topographic variables with SCP area, it should be highlighted that spatial correlation analysis of these variables and % SCP shows no statistical significance using all grids. Thus, as might be expected, these variables are only part of the motivation for SCP implementation and other factors are also important on the SCP adoption, such as governmental regulations, farm profitability, knowledge, tools and management. Also, this mapping is only focused on vegetative/structural practices, but there are many practices that are able to be implemented in regions with potential erosion problems as well.

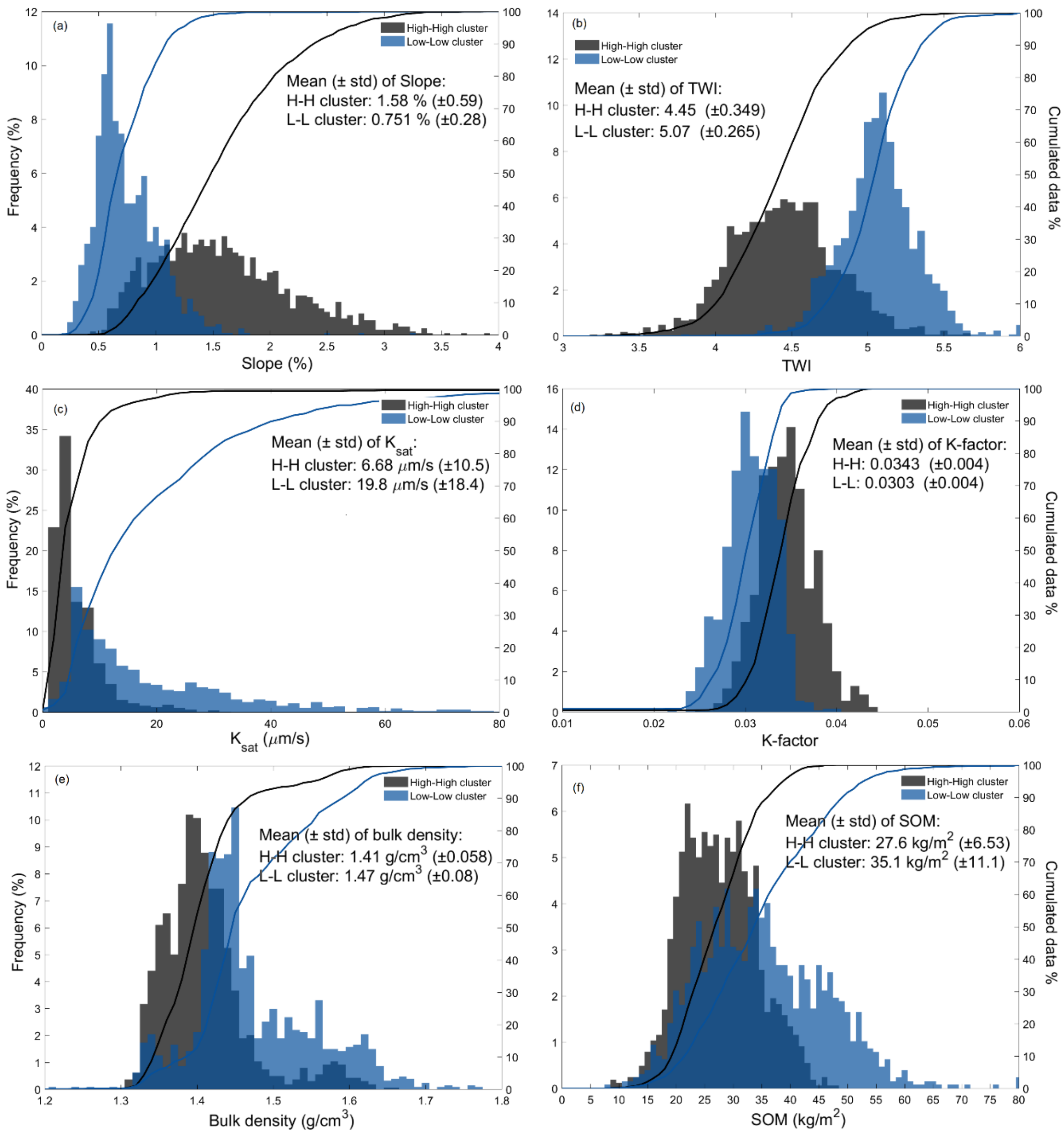

Fig. 6. Histograms of the soil and elevation-related properties within high-high and low-low clusters of SCPs. (a) slope, (b) topographic wetness index, (c) saturated hydraulic conductivity, (d) soil erodibility factor (e) bulk density, and (f) soil organic matter. The brief description of these variables is described in Section 2.5. The mapping areas of high-high and low-low clusters is presented in the Fig. 5.

When one compares the spatial pattern of potential soil erosion and % SCP values in Fig. 7, the conservation efforts by farmers in high soil risk areas are evident. The histogram also shows the higher erosion values (average: 8.82 tons/ha/year) in the high-high cluster of SCP areas compared to low-low cluster (average: 3.34 tons/ha/year). Since this result highlights the spatial overlap of high erosion and high SCP areas, an interesting observation should be made in this result. The soil erosion modeling indicates the potential erosion according to climate-topographic conditions of the region, disregarding conservation practice implementation. In contrast, the classified SCP areas illustrates the action of farmers by adopting vegetative/structural practices to minimize the erosion impacts. Thus, the real erosion rate is likely different and needs to incorporate spatially explicit information about conservation practices. Another insight on this result is the assessment of counties with conservation needs (↑ soil erosion, ↓ SCP areas), such as Cedar/Nebraska, Crawford/ Iowa, Shelby/Iowa, and Seward/Nebraska.

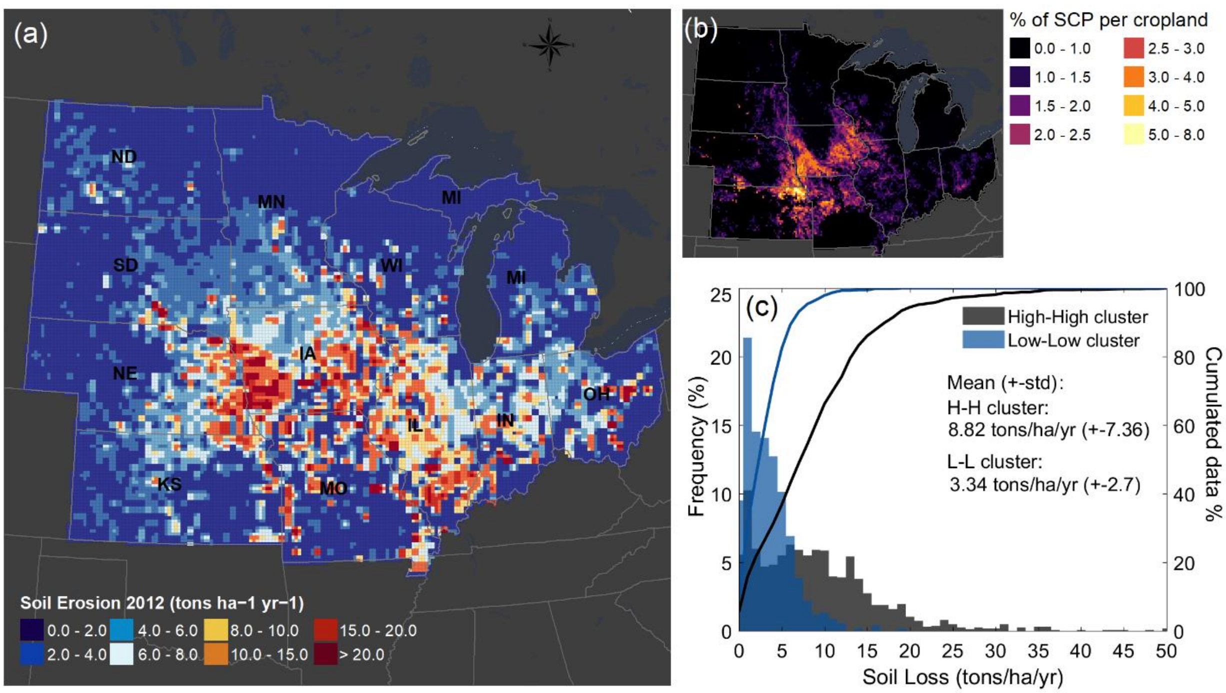

Fig. 7. Spatial distribution of soil erosion rates and its distribution within high-high/low-low clusters of SCPs. (a) Soil erosion 2012 map from Borrelli et al. (2017), (b) Spatial distribution of % SCP in agricultural areas as presented in Fig. 5, (c) Histogram of soil erosion values within high-high and low-low clusters of SCPs. U.S. state abbreviations: Illinois (IL), Indiana (IN), Iowa (IA), Kansas (KS), Michigan (MI), Minnesota (MN), Missouri (MO), Nebraska (NE), North Dakota (ND), Ohio (OH), South Dakota (SD), Wisconsin (WI).

4. Discussion

4.1. Mapping of structural conservation practices

This study performed the first automated mapping of SCP areas in Midwest U.S. croplands using NAIP aerial imagery (2018-2019). So far, there is no study that provides a spatially explicit mapping of these practices for the entire region, and the results give insights about conservation efforts from landowners. The results shown in Fig. 3 and S3 illustrate the suitability of adapted U-Net algorithm, and the mapping achieved the overall accuracy of 78.2% across 20 counties (Table 1). In general, the results reveal a large difference in SCP occurrence across Midwest states (Fig. 4), and spatial distribution shows some patterns in the SCP extent (Fig. 5). For instance, our findings illustrate that southwest Iowa, northeast Kansas and east Nebraska present the highest percentage of SCPs per cropland areas, while central Iowa (Des Moines Lobe) presents an intense agricultural area with low percentage of SCP areas (< 1% of SCP in cropland). Further, we observed that Illinois presents near-similar magnitude of SCP areas. In the visual inspection, we observed that some regions have a high number of terraces in the croplands such as Kansas. In contrast, the grassed waterways were vastly classified in the Iowa and Illinois. Historically, terraces and grasslands are well-recognized for reducing runoff and sediment delivery from agricultural areas (Fiener and Auerswald, 2003; Tarolli et al., 2014), and this final product allowed the quantification of these two practices across these states.

Regarding the spatial pattern (Fig. 5), the results show slight differences between soil and topographic-related variables between high-high and low-low cluster of SCP areas, such as slope and saturated hydraulic conductivity (Fig. 6). These results suggest that regional landscape characteristics and risk perceptions can potentially influence on the farmer actions. Several studies have performed meta-analysis to understand the motivations and barriers for farmer's adoption of BMPs (Prokopy et al., 2008; Jackson-Smith et al., 2010; Baumgart-Getz et al., 2012). The local network, conservation adoption by neighbors, and geophysical characteristics of the land (soil properties, slope) are listed as potential factors (see review in Liu et al. (2018)). Likewise, Baumgart-Getz et al. (2012) showed that access to information, financial capacity, and being connected to agency or watershed groups have impact on farmer motivation. In this topic, the evaluation of existing practices and social surveys might support the understanding of farmer needs and attitudes in support to conservation practices.

4.2. Implications for conservation programs

As part of U.S. Farm Bill support, conservation programs have broadly encouraged farmers to adopt BMPs (Reimer, 2015) through directives as Environmental Quality Incentives Program, and Conservation Stewardship Program. These financial and technical assistance programs have become an essential mechanism for promoting conservation among farmers and rural landowners (Reimer and Prokopy, 2014). According to Resources Conservation Act report (RCA, 2020), Iowa NRCS programs have supported the adoption of 32,674 terraces and 38,877 grassed waterways between 2005 and 2019. Until now, this information is primarily available on historical records (tabular) or local\regional projects such as Iowa BMP project. Although formal conservation program records are useful for general insights (Fig. 4), they are typically limited in the monitoring of successful degree of SCP implementation. Jackson-Smith et al. (2010) mentioned the need of efficient tracking system for monitoring the funded contracts after implementation of SCPs, which may help a better understanding of long-term consequences of these cost-share programs. In this context, the quantitative assessment of SCP areas can have positive implications for these programs. For example, conservation program managers can use this geospatial inventory to follow-up the farmer's actions and the consolidation of sponsored projects. In addition, these results are useful to advertise the positive environmental outcomes achieved by these programs. Another benefit is the evaluation of SCP distribution to support the decision of future projects. By understanding the location of current practices and conservation needs, new contracts and priority areas can be determined. In these efforts, the application of ACPF tool becomes essential to identify the preferential locations for certain practices (Tomer et al., 2013). However, Rundhaug (2018) showed at least 78% of potential grassed waterways from ACPF results were already implemented in three Iowa watersheds. This is a positive validation for ACPF method, but it also showed the importance of integration of existing practices to improve the watershed conservation plan prior to implementation of project. With long-term environmental goals, the combination of all these factors (conservation plan, financial incentives, information) can influence on farmers' actions (Carlisle, 2016).

Regarding the impacts on northern Gulf of Mexico zone, U.S. NRCS has supported different initiatives to reduce the nitrogen and phosphorus loads into surface waters of Mississippi River watershed, such as Mississippi River Basin Healthy Watersheds Initiative. The regional and local efforts have improved the water quality in some sub-watersheds of Mississippi River watershed (McLellan et al., 2015; Garcia et al., 2016; Leh et al., 2018), but others have increased the nutrient yields and the previous goal of Gulf of Mexico hypoxic zone (5-yr average areal extent < 5,000 km^2) was extended to the year 2035 (Rabalais and Turner, 2019). While some studies and technical reports have shown the benefits of SCPs based on field experiments and simulations (Yuan et al., 2002; Fiener and Auerwald, 2005; Dermisis et al., 2010; Iowa NRS, 2019), the conservation impact is often difficult to quantify in large watersheds. Tomer and Locker (2011) stated that Conservation Effects Assessment Project (CEAP) faced the problem of validating the impact of conservation in the water quality because large agricultural watersheds include a mix of practices and it is difficult to isolate the effect of individual actions. In addition, the cost effectiveness of a given practice is dependent on several factors, such as terrain condition, soil type, cropping systems, field location (adjacent to streams), and combination of other practices (Czapar et al., 2005; Zhou et al., 2009). These aspects show that only SCP mapping does not explain the trade-off between existing practices and environmental outcomes, and further research is needed on cost-effective targeting of conservation investments to understand the real impact of such practices in different crop fields (Maresch et al., 2008; Rabotyagov et al., 2014).

4.3. Implications for soil erosion and runoff modeling

The structural conservation practices are directly related to efforts on soil erosion control and reduction of nutrient loss from agricultural lands (Xiong et al., 2018), and this mapping allows further discussion of soil-related issues. In general, our results show that most counties with high erosion-prone areas have large extent of SCP areas (Fig. 7), suggesting the conservation efforts have paid off with implementation by farmers. Previous studies that have shown high soil erosion rates in the Midwest U.S. region (Doetterl et al., 2012; Borrelli et al., 2017; Tan et al., 2020) but they have poorly considered conservation practice P factor into soil erosion estimates (Xiong et al., 2018). As discussed by Panagos et al. (2015) and Sartori et al. (2019), P-factor is one of the most uncertain and difficult pieces of information to access. Naipal et al. (2015) recognized the importance of P-factor in local variation of soil erosion but they did not consider the P-factor due to data limitation on a global scale. More recently, Xiong et al. (2019) stated that P-factor datasets are relevant to improve soil erosion modeling and advanced image processing techniques should be considered to fill the knowledge gap for large-area projects. While additional processing is required to convert this mapping product into P-factor values (Wang et al., 2016), the proposed mapping of SCPs brings a new opportunity for further improvements of soil erosion maps and risk scenarios promoted by agricultural activities in the Midwest region. The Daily Erosion Project (Gelder et al., 2017), a WEPP (Flanagan and Nearing, 1995) based erosion model, includes terraces to the extent that they subdivide a hillslope into distinct overland flow elements, however it neglects contour buffer strips as they are too small to be captured in the USDA CDL, and thus the ACPF database. In a similar context, accurate modeling of surface management practices as well as surface runoff volumes and peak runoff rates influences erosion and entrainment of pollutants, which enables modeling of the load reduction goals of a pollutant to meet water quality standards. Thus, field-level analysis of SCPs can potentially improve the runoff estimates as they consider the practices affecting this process (Lee et al., 2010). This study has no intention to explore these modeling aspects, but this discussion illustrates potential benefits and applications of the SCP product.

4.4. Advantages and limitations of this framework

As discussed in other studies (Garcia-Garcia et al., 2018; Guo et al., 2018), the successful application of semantic segmentation methods requires significant computational resources. The implemented U-Net model has a deeper architecture and large input size (256 x 256 pixels), and the training process took 13 days with large GPU memory (32 GB). Users/developers should be aware of these requirements when they decide to implement semantic segmentation method. In addition, the ability to quantify SCP areas using a regional-scale algorithm is also a challenge, and a more general model is required. The high number of SCP areas across Iowa introduces the variability of SCP conditions (orientation, size, and shapes) in the training dataset, and the results show that 500,000 samples give such generalization for this application. Conceptually, the mapping presented in this study assumes that spatial-spectral patterns of SCP areas are visually identifiable in the optical images. Once the model recognizes these patterns, we can classify the new areas using adequate spatial resolution. Following that, medium spatial resolution data such as Sentinel-2 MSI and Landsat-8 OLI are not suitable for this application but commercial satellites can be considered in other countries, such as PlanetScope from Planet Labs and WorldView-4 from DigitalGlobe. In the same context, large-area application of high spatial resolution data often implies on high spatial detail and heterogenous landscape and our assumption of visual detection of SCP areas might not hold in some areas due to small difference of spatial-spectral features between cropland and SCP areas. Also, we observed that terraces and grassed waterways can be confused with other features. For instance, false-positive areas were observed in the irrigated systems, wetter areas, and cropland with non-homogeneous surface (Fig. S4). In contrast, false negative results showed that SCP areas were potentially underestimated in this product, which illustrated the importance of this preliminary assessment for further improvements of the methodology. Recognizing these limitations, our findings should be interpreted with caution at farm-level because we did not conduct a manual editing of this product, and the visual inspection is recommended when applied for specific farmland.

In addition, this study presents a binary map of SCP areas for overview distribution in the entire region, but some researchers can be more interested in multi-class records. This semantic segmentation with three false-color bands does not allow accurate distinction of SCP types since the spectral/spatial features are quite similar in some cases, such as grassed terraces versus narrow waterways. Also, users should notice that other practices were eventually classified in this product, such as filter strips and riparian buffer zone. As mentioned, SCP classification requires high spatial resolution data for target identification, and the data availability imposes limitations for further improvements in this large-area application. For example, a potential improvement (not proven) in this classification is the addition of topographic variables such as hillshade. However, high-resolution elevation models are only available for some states, and they have different quality protocols, vertical accuracy and time of acquisition. These differences impede achieving reliable and comparable results among states, and our classification framework does not include these LiDAR-derived data to avoid potential bias in the overall analysis. Beyond that, improvements to the current study could be explored with the extension of this methodology by including new labeled samples from other states, evaluation of other deep learning methods, post-processing with manual editing, and classification strategies for statewide projects with high-resolution LiDAR data. While this discussion highlights aspects to be improved, these preliminary results have shown a promising framework.

5. Conclusion

This study presented the first mapping of structural conservation practice over Midwest United States croplands. These preliminary results indicated the potential of this framework for regional monitoring of SCP areas using the adapted U-Net model and NAIP imagery (2018-2019). In general, SCP mapping achieved 78.2% of overall accuracy, but false-negative results showed underestimation of SCP areas (recall: 53.3%). The results showed large variability in SCP occurrence among Midwest states, with high occurrence in Iowa, Kansas, Illinois and Nebraska. In contrast, Michigan, North Dakota, and Minnesota presented the lowest percentage of SCP in their croplands. Overall, we observed that clusters of SCP areas are associated with certain soil and terrain conditions: high-high clusters of SCPs were observed in the slope higher than 1.5 %, bulk density lower than 1.4 g/cm^3, and K_{sat} lower than 7 µm/s. Our findings also showed the agreement in the spatial pattern of SCP areas and high erosion-prone areas, which documents farmer efforts towards soil conservation. Although preliminary analysis shows the applicability of this framework, the farm-level analysis requires some cautions since there are known source of errors such as discontinuity or mislabeling of SCP areas. We encourage further experiments with additional input sources such as terrain-derived information for local-scale mapping. Finally, a spatially explicit inventory of SCP areas is useful for a variety of scientific and policy applications such as (i) the understanding of farmer's contribution for soil and water conservation, (ii) the improvement of soil erosion risk modeling by considering structural conservation practices, and (iii) the evaluation of priority areas by national programs. Considering the importance of soil and water conservation in agricultural areas, this framework using semantic segmentation model becomes a promising approach for further assessment of these practices in the Midwest U.S. croplands.

Acknowledgements

We thank the USDA's Farm Service Agency (FSA) for publicly NAIP imagery, and other USDA resources for accomplishment of this study. The national cropland product is available at https://nassgeodata.gmu.edu/CropScape/. We thank the California Soil Resource Lab for the availability of soil products (https://casoilresource.lawr.ucdavis.edu/). We also thank the JRC\ESDAC for the availability of Global Soil Erosion map from Borrelli et al. (2017) (https://esdac.jrc.ec.europa.eu/content/global-soil-erosion). Also, Iowa BMP project was a key resource for this study (https://www.gis.iastate.edu/gisf/projects/conservation-practices), and we thank Robin McNeely for sharing the geodatabase. This study used the ISU high performance computing resources (https://www.hpc.iastate.edu/), and we thank the HPC team for available resources.

References

Badrinarayanan, V., Kendall, A., and Cipolla, R. (2017). Segnet: A deep convolutional encoder-decoder architecture for image segmentation. IEEE transactions on pattern analysis and machine intelligence, 39(12), 2481-2495.

Basu, S., Ganguly, S., Nemani, R. R., Mukhopadhyay, S., Zhang, G., Milesi, C., ... and Cook, B. (2015). A semiautomated probabilistic framework for tree-cover delineation from 1-m NAIP imagery using a high-performance computing architecture. IEEE Transactions on Geoscience and Remote Sensing, 53(10), 5690-5708.

Baumgart-Getz, A., Prokopy, L. S., and Floress, K. (2012). Why farmers adopt best management practice in the United States: A meta-analysis of the adoption literature. Journal of environmental management, 96(1), 17-25.

Borrelli P., Robinson D.A., Fleischer L.R., Lugato E., Ballabio C., Alewell C., Meusburger K., Modugno, S., Schutt, B. Ferro, V. Bagarello, V. Van Oost, K., Montanarella, L., Panagos P. 2017. An assessment of the global impact of 21st century land use change on soil erosion. Nature Communications, 8 (1): art. no. 2013

Carlisle, L. (2016). Factors influencing farmer adoption of soil health practices in the United States: A narrative review. Agroecology and Sustainable Food Systems, 40(6), 583-613.

Carpenter, S. R., Caraco, N. F., Correll, D. L., Howarth, R. W., Sharpley, A. N., and Smith, V. H. (1998). Nonpoint pollution of surface waters with phosphorus and nitrogen. Ecological applications, 8(3), 559-568.

Cochran, W. G. (2007). Sampling techniques. John Wiley and Sons.

Congalton, R. G. (1991). A review of assessing the accuracy of classifications of remotely sensed data. Remote sensing of environment, 37(1), 35-46.

Czapar, G.F., J.M. Laflen, G.F. McIsaac, and D.P. McKenna. (2005). Effects of erosion control practices on nutrient loss. In Final Report: Gulf Hypoxia and Local Water Quality Concerns Workshop, Ames, Iowa, September 26-28, 117-127. Ames, IA: Upper Mississippi River Sub-basin Hypoxia Nutrient Committee.

Dale, V. H., Armitage, T., Bianchi, T., Blumberg, A., Boynton, W., Conley, D. J., ... and Kling, C. L. (2010). Hypoxia in the northern Gulf of Mexico. New York: Springer.

Delgado, J. A., Groffman, P. M., Nearing, M. A., Goddard, T., Reicosky, D., Lal, R., ... and Salon, P. (2011). Conservation practices to mitigate and adapt to climate change. Journal of soil and water conservation, 66(4), 118A-129A.

Dermisis, D., Abaci, O., Papanicolaou, A. N., and Wilson, C. G. (2010). Evaluating grassed waterway efficiency in southeastern Iowa using WEPP. Soil Use and Management, 26(2), 183-192.

Diaz, R. J., and Rosenberg, R. (2008). Spreading dead zones and consequences for marine ecosystems. science, 321(5891), 926-929.

Doetterl, S., Van Oost, K., and Six, J. (2012). Towards constraining the magnitude of global agricultural sediment and soil organic carbon fluxes. *Earth Surface Processes and Landforms*, *37*(6), 642-655.

Fiener, P., and Auerswald, K. (2003). Effectiveness of grassed waterways in reducing runoff and sediment delivery from agricultural watersheds. Journal of Environmental Quality, 32(3), 927-936.

Fiener, P., and Auerswald, K. (2005). Measurement and modeling of concentrated runoff in grassed waterways. Journal of Hydrology, 301(1-4), 198-215.

Flanagan, D. C., and Nearing, M. A. (1995). USDA-Water Erosion Prediction Project: Hillslope profile and watershed model documentation. National Soil Erosion Research Laboratory Report # 10, 1-123.

Floress, K., Reimer, A., Thompson, A., Burbach, M., Knutson, C., Prokopy, L., ... and Ulrich-Schad, J. (2018). Measuring farmer conservation behaviors: Challenges and best practices. Land use policy, 70, 414-418.

Friedrich, T., Derpsch, R., and Kassam, A. (2012). Overview of the global spread of conservation agriculture. Field Actions Science Reports. The journal of field actions, (Special Issue 6).

García, A. M., Alexander, R. B., Arnold, J. G., Norfleet, L., White, M. J., Robertson, D. M., and Schwarz, G. (2016). Regional effects of agricultural conservation practices on nutrient transport in the Upper Mississippi River Basin. Environmental science and technology, 50(13), 6991-7000.

Garcia-Garcia, A., Orts-Escolano, S., Oprea, S., Villena-Martinez, V., Martinez-Gonzalez, P., and Garcia-Rodriguez, J. (2018). A survey on deep learning techniques for image and video semantic segmentation. Applied Soft Computing, 70, 41-65.

Gelder, B., Sklenar, T., James, D., Herzmann, D., Cruse, R., Gesch, K., and Laflen, J. (2018). The Daily Erosion Project–daily estimates of water runoff, soil detachment, and erosion. Earth Surface Processes and Landforms, 43(5), 1105-1117.

Guo, Y., Liu, Y., Georgiou, T., and Lew, M. S. (2018). A review of semantic segmentation using deep neural networks. *International journal of multimedia information retrieval*, *7*(2), 87-93.

Haas, M. B., Guse, B., and Fohrer, N. (2017). Assessing the impacts of Best Management Practices on nitrate pollution in an agricultural dominated lowland catchment considering environmental protection versus economic development. Journal of environmental management, 196, 347-364.

Hobbs, P. R., Sayre, K., and Gupta, R. (2007). The role of conservation agriculture in sustainable agriculture. Philosophical Transactions of the Royal Society B: Biological Sciences, 363(1491), 543-555.

Iowa Corn (2019). Iowa corn promotion board. https://www.iowacorn.org. Accessed April 20, 2019.

Iowa NRS (2019). Iowa Nutrient Reduction Strategy 2018-19 Annual Progress Report. Iowa State University, Iowa Department of Agriculture and Land Stewardship (IDALS), Iowa Dept. of Natural Resources. Ames: Iowa State University.

ISU GIS Facility. (2016). Iowa BMP Mapping Project: Download Iowa Conservation Practices by HUC-12. Available at https://www.gis.iastate.edu/gisf/projects/conservation-practices. Accessed April 15, 2020.

ISU-IBMP. 2017. Iowa Best Management Practices (BMP) mapping project handbook. https://www.iowaview.org/wp-content/uploads/2018/03/Iowa-Best-Management-Practices-Mapping-Handbook.pdfl. Accessed Oct. 29, 2020.

Jackson-Smith, D. B., Halling, M., de la Hoz, E., McEvoy, J. P., and Horsburgh, J. S. (2010). Measuring conservation program best management practice implementation and maintenance at the watershed scale. Journal of Soil and Water Conservation, 65(6), 413-423.

Jat, R. A., Sahrawat, K. L., and Kassam, A. H. (Eds.). (2013). Conservation agriculture: global prospects and challenges. Cabi.

Jégou, S., Drozdzal, M., Vazquez, D., Romero, A., and Bengio, Y. (2017). The one hundred layers tiramisu: Fully convolutional densenets for semantic segmentation. In Proceedings of the IEEE Conference on Computer Vision and Pattern Recognition Workshops (pp. 11-19).

Kassam, A., Friedrich, T., and Derpsch, R. (2019). Global spread of conservation agriculture. International Journal of Environmental Studies, 76(1), 29-51.

Kassam, A., Friedrich, T., Shaxson, F., and Pretty, J. (2009). The spread of conservation agriculture: justification, sustainability and uptake. International journal of agricultural sustainability, 7(4), 292-320.

Knowler, D., and Bradshaw, B. (2007). Farmers' adoption of conservation agriculture: A review and synthesis of recent research. Food policy, 32(1), 25-48.

Kröger, R., Dunne, E. J., Novak, J., King, K. W., McLellan, E., Smith, D. R., ... and Noe, G. B. (2013). Downstream approaches to phosphorus management in agricultural landscapes: regional applicability and use. Science of the Total Environment, 442, 263-274.

Kröger, R., Perez, M., Walker, S., and Sharpley, A. (2012). Review of best management practice reduction efficiencies in the Lower Mississippi Alluvial Valley. Journal of soil and water conservation, 67(6), 556-563.

Lam, Q. D., Schmalz, B., and Fohrer, N. (2011). The impact of agricultural Best Management Practices on water quality in a North German lowland catchment. Environmental monitoring and assessment, 183(1-4), 351-379.

Lee, M., Park, G., Park, M., Park, J., Lee, J., and Kim, S. (2010). Evaluation of non-point source pollution reduction by applying Best Management Practices using a SWAT model and QuickBird high resolution satellite imagery. Journal of Environmental Sciences, 22(6), 826-833.

Leh, M. D., Sharpley, A. N., Singh, G., and Matlock, M. D. (2018). Assessing the impact of the MRBI program in a data limited Arkansas watershed using the SWAT model. Agricultural water management, 202, 202-219.

Lewandowski, A. M., Tomer, M. D., Buchanan, J. I., Kiel, A., Olson, L., Power, R. L., and Sloan, J. J. (2020). Agricultural Conservation Planning Framework: Watershed applications, research opportunities, and training resources. *Journal of Soil and Water Conservation*.

Liu, R., Zhang, P., Wang, X., Chen, Y., and Shen, Z. (2013). Assessment of effects of best management practices on agricultural non-point source pollution in Xiangxi River watershed. Agricultural Water Management, 117, 9-18.

Liu, T., Bruins, R. J., and Heberling, M. T. (2018). Factors influencing farmers' adoption of best management practices: A review and synthesis. Sustainability, 10(2), 432.

Liu, Y., Engel, B. A., Flanagan, D. C., Gitau, M. W., McMillan, S. K., and Chaubey, I. (2017). A review on effectiveness of best management practices in improving hydrology and water quality: Needs and opportunities. Science of the Total Environment, 601, 580-593.

Long, J., Shelhamer, E., and Darrell, T. (2015). Fully convolutional networks for semantic segmentation. In Proceedings of the IEEE conference on computer vision and pattern recognition (pp. 3431-3440).

Maresch, W., Walbridge, M. R., and Kugler, D. (2008). Enhancing conservation on agricultural landscapes: A new direction for the Conservation Effects Assessment Project. journal of soil and water conservation, 63(6), 198A-203A.

Martins, V. S., Kaleita, A. L., Gelder, B. K., da Silveira, H. L., & Abe, C. A. (2020). Exploring multiscale object-based convolutional neural network (multi-OCNN) for remote sensing image classification at high spatial resolution. *ISPRS Journal of Photogrammetry and Remote Sensing*, *168*, 56-73.

McLellan, E., Robertson, D., Schilling, K., Tomer, M., Kostel, J., Smith, D., and King, K. (2015). Reducing nitrogen export from the Corn Belt to the Gulf of Mexico: Agricultural strategies for remediating hypoxia. JAWRA Journal of the American Water Resources Association, 51(1), 263-289.

Naipal, V., Reick, C. H., Pongratz, J., and Van Oost, K. (2015). Improving the global applicability of the RUSLE model-adjustment of the topographical and rainfall erosivity factors. *Geoscientific Model Development*, *8*, 2893-2913.

Panagopoulos, Y., Makropoulos, C., and Mimikou, M. (2011). Reducing surface water pollution through the assessment of the cost-effectiveness of BMPs at different spatial scales. Journal of environmental management, 92(10), 2823-2835.

Panagos, P., Borrelli, P., Meusburger, K., van der Zanden, E. H., Poesen, J., and Alewell, C. (2015). Modelling the effect of support practices (P-factor) on the reduction of soil erosion by water at European scale. Environmental science and policy, 51, 23-34.

Panagos, P., Van Liedekerke, M., Jones, A., and Montanarella, L. (2012). European Soil Data Centre: Response to European policy support and public data requirements. *Land use policy*, *29*(2), 329-338.

Peter, J., Hogland, J., Anderson, N., Drake, J., and Medley, P. (2018). Fine resolution probabilistic land cover classification of landscapes in the southeastern United States. ISPRS International Journal of Geo-Information, 7(3), 107.

Prokopy, L. S., Floress, K., Klotthor-Weinkauf, D., and Baumgart-Getz, A. (2008). Determinants of agricultural best management practice adoption: Evidence from the literature. Journal of soil and water conservation, 63(5), 300-311.

Quinn, P. F., Beven, K. J., and Lamb, R. (1995). The in (a/tan/β) index: How to calculate it and how to use it within the topmodel framework. *Hydrological processes*, *9*(2), 161-182.

Rabalais, N. N., and Turner, R. E. (2019). Gulf of Mexico hypoxia: Past, present, and future. Limnology and Oceanography Bulletin, 28(4), 117-124.

Rabalais, N. N., Turner, R. E., and Scavia, D. (2002). Beyond Science into Policy: Gulf of Mexico Hypoxia and the Mississippi River: Nutrient policy development for the Mississippi River watershed reflects the accumulated scientific evidence that the increase in nitrogen loading is the primary factor in the worsening of hypoxia in the northern Gulf of Mexico. BioScience, 52(2), 129-142.

Rabotyagov, S. S., Campbell, T. D., White, M., Arnold, J. G., Atwood, J., Norfleet, M. L., ... and Turner, R. E. (2014). Cost-effective targeting of conservation investments to reduce the northern Gulf of Mexico hypoxic zone. Proceedings of the National Academy of Sciences, 111(52), 18530-18535.

RCA (2020). NRCS Conservation Programs. https://www.nrcs.usda.gov/Internet/NRCS_RCA/reports/cp_ia.html. Accessed May 1, 2020.

Reimer, A. (2015). Ecological modernization in US agri-environmental programs: Trends in the 2014 Farm Bill. Land Use Policy, 47, 209-217.

Reimer, A. P., and Prokopy, L. S. (2014). Farmer participation in US Farm Bill conservation programs. *Environmental management*, *53*(2), 318-332.

Reimer, A. P., Weinkauf, D. K., and Prokopy, L. S. (2012). The influence of perceptions of practice characteristics: An examination of agricultural best management practice adoption in two Indiana watersheds. Journal of Rural Studies, 28(1), 118-128.

Ronneberger, O., Fischer, P., and Brox, T. (2015, October). U-net: Convolutional networks for biomedical image segmentation. In International Conference on Medical image computing and computer-assisted intervention (pp. 234-241). Springer, Cham.

Rundhaug, T. J., Geimer, G. R., Drake, C. W., Amado, A. A., Bradley, A. A., Wolter, C. F., and Weber, L. J. (2018). Agricultural conservation practices in Iowa watersheds: comparing actual implementation with practice potential. Environmental monitoring and assessment, 190(11), 659.

Sartori, M., Philippidis, G., Ferrari, E., Borrelli, P., Lugato, E., Montanarella, L., and Panagos, P. (2019). A linkage between the biophysical and the economic: Assessing the global market impacts of soil erosion. *Land Use Policy*, *86*, 299-312.

Schoumans, O. F., Chardon, W. J., Bechmann, M. E., Gascuel-Odoux, C., Hofman, G., Kronvang, B., ... and Dorioz, J. M. (2014). Mitigation options to reduce phosphorus losses from the agricultural sector and improve surface water quality: a review. Science of the Total Environment, 468, 1255-1266.

Schumann, G. J., and Bates, P. D. (2018). The need for a high-accuracy, open-access global DEM. Frontiers in Earth Science, 6, 225.

Stoddard, J. L., Van Sickle, J., Herlihy, A. T., Brahney, J., Paulsen, S., Peck, D. V., ... and Pollard, A. I. (2016). Continental-scale increase in lake and stream phosphorus: Are oligotrophic systems disappearing in the United States?. Environmental science and technology, 50(7), 3409-3415.

Stoian, A., Poulain, V., Inglada, J., Poughon, V., and Derksen, D. (2019). Land cover maps production with high resolution satellite image time series and convolutional neural networks: Adaptations and limits for operational systems. Remote Sensing, 11(17), 1986.

Strahler, A. H., Boschetti, L., Foody, G. M., Friedl, M. A., Hansen, M. C., Herold, M., ... and Woodcock, C. E. (2006). Global land cover validation: Recommendations for evaluation and accuracy assessment of global land cover maps. European Communities, Luxembourg, 51(4).

Tan, Z., Leung, L. R., Li, H. Y., Tesfa, T., Zhu, Q., and Huang, M. (2020). A substantial role of soil erosion in the land carbon sink and its future changes. Global Change Biology, 26(4), 2642-2655.

Tarolli, P., Preti, F., and Romano, N. (2014). Terraced landscapes: From an old best practice to a potential hazard for soil degradation due to land abandonment. Anthropocene, 6, 10-25.

Tomer, M. D., and Locke, M. A. (2011). The challenge of documenting water quality benefits of conservation practices: A review of USDA-ARS's conservation effects assessment project watershed studies. Water Science and Technology, 64(1), 300-310.

Tomer, M. D., Porter, S. A., Boomer, K. M. B., James, D. E., Kostel, J. A., Helmers, M. J., ... and McLellan, E. (2015). Agricultural conservation planning framework: 1. Developing multipractice watershed planning scenarios and assessing nutrient reduction potential. Journal of environmental quality, 44(3), 754-767.

Tomer, M. D., Porter, S. A., James, D. E., Boomer, K. M., Kostel, J. A., and McLellan, E. (2013). Combining precision conservation technologies into a flexible framework to facilitate agricultural watershed planning. Journal of Soil and Water Conservation, 68(5), 113A-120A.

Triplett Jr, G. B., and Dick, W. A. (2008). No-tillage crop production: A revolution in agriculture!. Agronomy journal, 100, S-153.

Tscharntke, T., Clough, Y., Wanger, T. C., Jackson, L., Motzke, I., Perfecto, I., ... and Whitbread, A. (2012). Global food security, biodiversity conservation and the future of agricultural intensification. Biological conservation, 151(1), 53-59.

Wagner, F. H., Sanchez, A., Aidar, M. P., Rochelle, A. L., Tarabalka, Y., Fonseca, M. G., ... and Aragão, L. E. (2020). Mapping Atlantic rainforest degradation and regeneration history with indicator species using convolutional network. *PloS one*, *15*(2), e0229448.

Wang, R., Zhang, S., Yang, J., Pu, L., Yang, C., Yu, L., ... and Bu, K. (2016). Integrated use of GCM, RS, and GIS for the assessment of hillslope and gully erosion in the Mushi River Sub-Catchment, Northeast China. *Sustainability*, *8*(4), 317.

Xiong, M., Sun, R., and Chen, L. (2018). Effects of soil conservation techniques on water erosion control: A global analysis. Science of the Total Environment, 645, 753-760.

Xiong, M., Sun, R., and Chen, L. (2019). Global analysis of support practices in USLE-based soil erosion modeling. Progress in Physical Geography: Earth and Environment, 43(3), 391-409.

Xu, Y., Wu, L., Xie, Z., and Chen, Z. (2018). Building extraction in very high resolution remote sensing imagery using deep learning and guided filters. Remote Sensing, 10(1), 144.

Yuan, Y., Dabney, S. M., and Bingner, R. L. (2002). Cost effectiveness of agricultural BMPs for sediment reduction in the Mississippi Delta. Journal of Soil and Water Conservation, 57(5), 259-267.

Zhang, X., and Zhang, M. (2011). Modeling effectiveness of agricultural BMPs to reduce sediment load and organophosphate pesticides in surface runoff. Science of the Total Environment, 409(10), 1949-1958.

Zhang, Z., Liu, Q., and Wang, Y. (2018). Road extraction by deep residual u-net. *IEEE Geoscience and Remote Sensing Letters*, *15*(5), 749-753.

Zhou, X., Al-Kaisi, M., and Helmers, M. J. (2009). Cost effectiveness of conservation practices in controlling water erosion in Iowa. Soil and Tillage Research, 106(1), 71-78.

Supplementary material

Digital mapping of structural conservation practices in the Midwest U.S. croplands: Implementation and preliminary analysis

Vitor S. Martins [a, b*], Amy L. Kaleita [a], Brian K. Gelder [a]

[a] Agricultural and Biosystems Engineering, Iowa State University, Ames, IA, United States.
[b] Center for Global Change and Earth Observations, Michigan State University, East Lansing, MI, United States.

* Corresponding author. E-mails: vitorsm@msu.edu (Vitor S. Martins)

Table S1. Characteristics of selected U.S. states and NAIP data used in the study.

States	State area	Cultivated area*	Annual rainfall	Elevation	Slope	NAIP imagery	
	km2		mm	m	%	Year	Size (GB)
Illinois (IL)	145,968	85,984	1071	191	1.10	2019	175.5
Indiana (IN)	93,789	45,498	1171	229	1.50	2018	108.0
Iowa (IA)	145,667	92,176	945	324	1.74	2019	134.4
Kansas (KS)	213,184	25,293	746	585	1.30	2019	188.6
Michigan (MI)	153,620	19,077	925	276	1.39	2018	172.0
Minnesota (MN)	218,781	62,952	740	371	1.20	2019	240.1
Missouri (MO)	180,431	32,733	1125	262	2.60	2018	190.1

Nebraska (NE)	200,365	58,572	623	795	1.75	2018	181.0
North Dakota (ND)	183,135	27,697	500	556	1.31	2019	175.0
Ohio (OH)	106,978	35,247	1096	283	2.60	2019	115.6
South Dakota (SD)	199,718	42,139	534	665	1.84	2018	196.2
Wisconsin (WI)	145,562	22,447	971	332	2.13	2018	107.2

* Corn and soybean areas were observed during more than five years between 2010-2019 in the NASS CDL program.

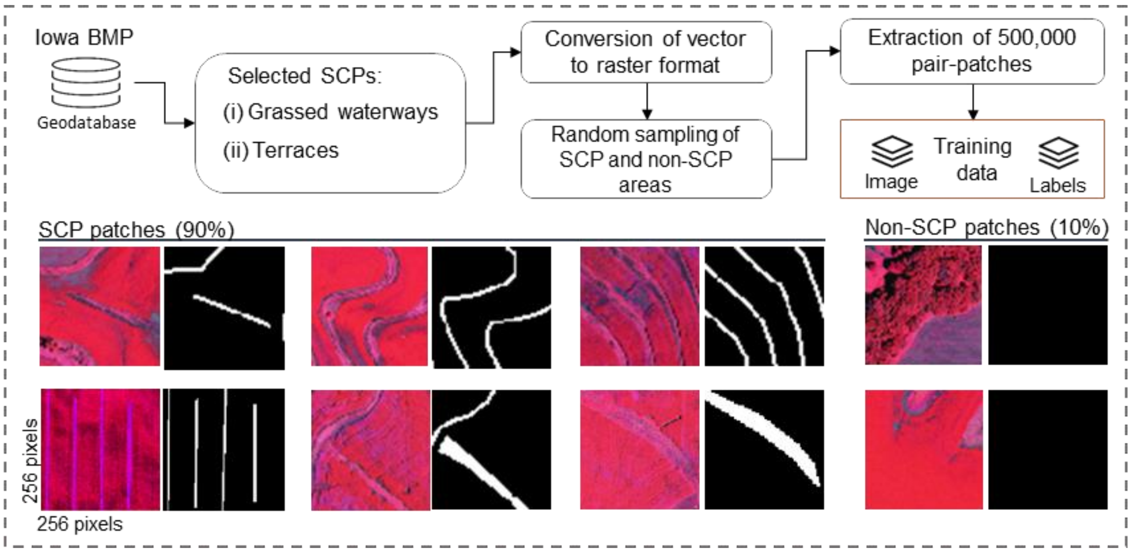

Fig. S1. Development of structural conservation practices (SCP) training dataset. The samples contain SCP (90%) and non-SCP (10%) patches obtained from Iowa BMP project.

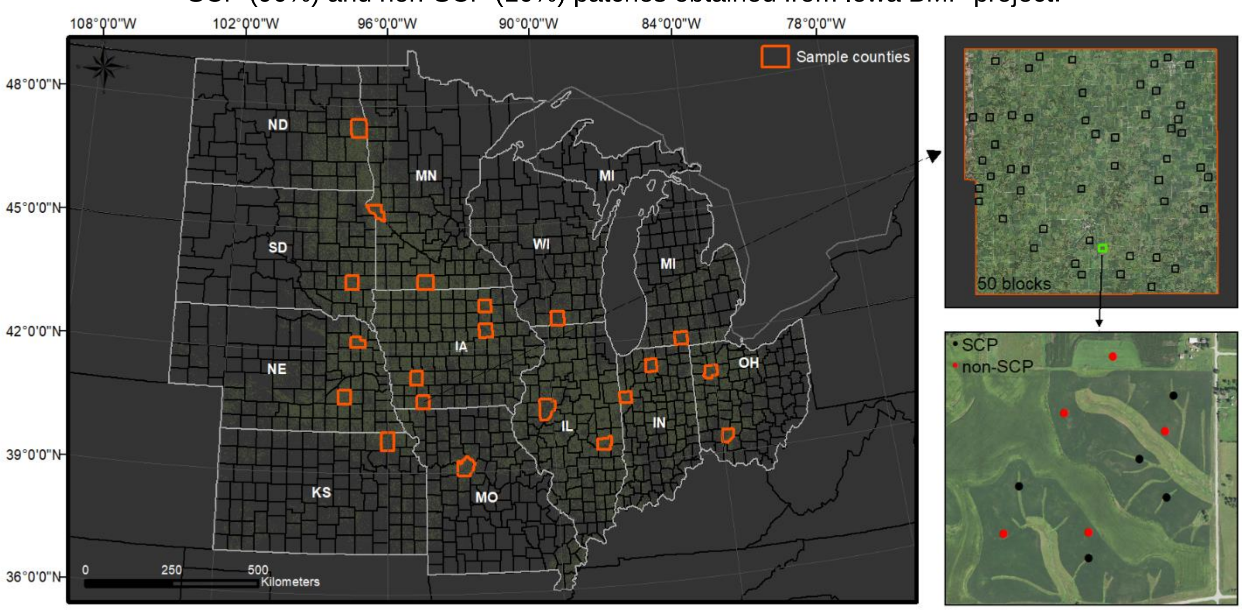

Fig. S2. Location of selected counties for validation procedure. *Top-right*: Distribution of 50 blocks across Taylor County, Iowa. *Bottom-right*: Examples of SCP/non-SCP samples for a specific block (green).

Fig. S3. Example of grassed waterways and terraces classification. *First row*: Grassed waterways (42.45°N, 91.56°W). *Second row*: Terraces (39.99°N, 96.41°W). The NAIP natural color images and local hillshade maps were illustrated in the right boxes.

Fig. S4. Examples of (a) omission and (b) commission problems in the classification results.